Journal of Sound and Vibration 328 (2009) 92–108

Contents lists available at ScienceDirect

Journal of Sound and Vibration

journal homepage: www.elsevier.com/locate/jsvi

Friction-induced vibration: Should low-order models be believed?

T. Butlin *, J. Woodhouse

Cambridge University Engineering Department, Trumpington Street, Cambridge CB2 1PZ, UK

ARTICLE INFO

Article history:
Received 4 May 2009
Received in revised form
13 July 2009
Accepted 3 August 2009
Handling Editor: H. Ouyang
Available online 26 August 2009

ABSTRACT

Much of the literature of friction-induced vibration focusses on highly simplified models that may include three or fewer modes to describe the independent subsystems. The degree to which these models approximate the behaviour of fuller models remains largely untested. This paper presents a systematic analysis of an example system to explore its convergence behaviour. First, the sensitivity to variations in contact parameters is considered, shedding light on the variability of experimental results. Second, the number of modes required for a 'minimal' model is explored. While three modes can often provide a reasonable local approximation to a more general model, the choice of which three is sometimes counter-intuitive. A method for automatic model reduction is proposed and found to be highly effective. The results challenge the general applicability of the oft-quoted two-degree-of-freedom model of 'mode-coupling', and also indicate some reasons for the difficulty encountered in validating models of friction-induced vibration.

1. Introduction

A wide variety of theoretical models has been developed to describe and predict friction-induced vibration. The literature on vehicle brake squeal has moved from very simple lumped-parameter models to ever more sophisticated finite element models, but experimental validation has proved difficult, suggesting that friction-coupled systems may be highly sensitive to parameter changes. This research has been summarised by North [1], Ibrahim and Rivin [2], Kinkaid et al. [3], Ouyang et al. [4] and Sheng [5]. Although detailed finite element models allow direct comparison with real systems, their inherent complexity can obscure underlying mechanisms and the relationship between system parameters and coupled behaviour. It is also hard to assess whether all relevant physical effects have been included in a model: FE methods cope well with geometric complexity, but less well with, for example, spatially varying damping or the more sophisticated varieties of frictional constitutive law. While a range of techniques exist to reduce FE models to fewer degrees of freedom (within the context of friction-induced vibration see for example Coudeyras [6], who use the method by Craig and Bampton [7]) it is not always clear in what sense the most significant dynamics have been retained from the perspective of friction-induced vibration.

For these reasons a significant proportion of the literature continues to focus on reduced-order models (e.g. Hoffmann et al. [8], Kinkaid [9], von Wagner [10] and Emira [11]). These provide a clearer insight into fundamental causes of instability, but their relationship to real systems is less direct. Claims have been made that one or another of these low-order models captures the essence of many, or most, cases of brake squeal instability, but how can one tell if such a claim is well-founded? This paper takes a modal view and considers how many modes of the 'disc' and 'brake' are needed to give a robust and reliable prediction of the full system behaviour over a limited frequency range. This study serves two functions: it tests

* Corresponding author. Tel.: +44 1223 748522.
E-mail addresses: tb267@cam.ac.uk (T. Butlin), jw12@cam.ac.uk (J. Woodhouse).

0022-460X/$ - see front matter © 2009 Elsevier Ltd. All rights reserved.
doi:10.1016/j.jsv.2009.08.001

the reliability of models of a given complexity and it sheds some light on the difficulties previously encountered in experimentally validating theoretical models.

The focus is on predicting linearised instability, not the subsequent nonlinear limit cycles, as the question of most interest within the context of vehicle brakes is usually whether or not squeal occurs. The model is currently limited to single-point contact systems but has the potential to be generalised to more complicated contact geometries. Modelling single-point contact systems is a logical starting point and the results are likely to form a subset of more complicated cases. The modal approach allows damping to be included throughout in a rather general way, and we also consider the effects of contact stiffness and linearised friction models. Gyroscopic effects are not considered here, but for an interesting discussion on this route to instability see Kirillov [12]. The experimental results associated with the present project were all carried out with low disc rotation speeds, and it might be hypothesised that gyroscopic effects were small.

In a previous paper, Butlin and Woodhouse [13] considered highly idealised models with just one, two and three modes under different modelling assumptions. It was demonstrated that high sensitivity with respect to parameter and modelling changes could occur under certain conditions and that predictions could be sensitive to parameters that are often neglected as insignificant. This makes it important to explore systematically the validity of predictions of a family of models, with a range of orders and modelling assumptions. The present paper addresses three specific questions:

- How sensitively does the predicted behaviour depend on modelling assumptions, particularly about the contact stiffness and the assumed frictional model?
- For a given set of these assumptions, over what bandwidth (if any) does a reduced-order model give a useful approximation to a complex system?
- What is the convergence behaviour of predictions as more modes are included in the system model?

It will emerge that these questions do not have simple answers. The objective of reduced-order models is to approximate over a limited frequency range a more complicated system having dynamics over a much wider bandwidth. The target here will be to identify 'minimal models' that give converged predictions over a bandwidth of interest without assuming *a priori* what level of complexity is required. Without this information, the usefulness of studying arbitrarily chosen low-order models is questionable. This study is an initial step in the wider context of a comparison between theoretical predictions and a large-scale experimental test (see Butlin and Woodhouse [14] and Butlin [15]).

2. Theoretical framework

The model is based on a linear transfer function analysis of two subsystems coupled by a sliding point contact. The general type of system to be analysed is sketched in Fig. 1. A 'disc' is driven at constant velocity, V_0, and a 'brake' is pushed against it with a dynamically varying normal force, N, composed of a steady equilibrium pre-load, N_0, plus a small fluctuating component, $N'e^{i\omega t}$, such that $N = N_0 + N'e^{i\omega t}$. Similarly, the force tangential to the sliding direction due to friction, F, can be expressed as a steady equilibrium force, F_0, plus a fluctuating component, $F'e^{i\omega t}$, such that $F = F_0 + F'e^{i\omega t}$. With a Coulomb friction law the normal and tangential forces are related by $F = \mu_0 N$ where μ_0 is the coefficient of friction. Consequently the sign of μ_0 defines the direction of rotation of the disc: if V_0 is positive then μ_0 is negative and vice versa. The normal and tangential displacements from equilibrium of the disc are denoted by u_1 and v_1, respectively, and u_2 and v_2 for the brake. The normal and tangential displacements from equilibrium of the point of contact are denoted by u_3 and v_3. The springs of stiffness k_n and k_t represent the linearised contact stiffness in the normal and tangential directions, respectively. Any damping that may result from the contact has been ignored.

The dynamics of the disc and brake, for this point-contact problem, can be described in terms of transfer functions:

$$\begin{bmatrix} u_1 \\ v_1 \end{bmatrix} = \begin{bmatrix} G_{11}(\omega) & G_{12}(\omega) \\ G_{21}(\omega) & G_{22}(\omega) \end{bmatrix} \begin{bmatrix} N' \\ F' \end{bmatrix} \tag{1}$$

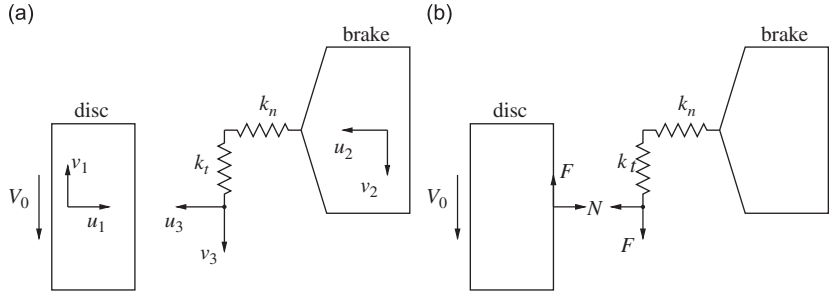

Fig. 1. Two linear subsystems coupled by a single point sliding contact with definition of variables. (a) Displacements. (b) Forces.

$$\begin{bmatrix} u_2 \\ v_2 \end{bmatrix} = \begin{bmatrix} H_{11}(\omega) & H_{12}(\omega) \\ H_{21}(\omega) & H_{22}(\omega) \end{bmatrix} \begin{bmatrix} N' \\ F' \end{bmatrix} \tag{2}$$

where $G_{ij}(\omega)$ represent the disc's response and $H_{ij}(\omega)$ represent the equivalent responses for the brake. These transfer functions can be determined using standard vibration measurement techniques. The convention of the vibration literature is followed by using transfer functions defined as the Fourier transform of an impulse response, rather than the Laplace transform. To convert to the Laplace formalism the complex ω-plane should be rotated anticlockwise by 90° to correspond to the complex s-plane as $s = \mathrm{i}\omega$.

The stability of the friction-coupled system can be determined from its transfer functions: all the poles of the transfer functions from any possible input to any output must be stable to predict overall stability. Assuming a constant coefficient of friction this leads to the characteristic function:

$$D = G_{11} + \mu_0 G_{12} + H_{11} + \mu_0 H_{12} + 1/k_n \tag{3}$$

as derived by Duffour and Woodhouse [16]. The system is stable if and only if all the zeros of $D(\omega)$ have a positive imaginary part. The corresponding condition for stability in the Laplace formalism would require all the zeros to lie in the left half-plane.

A common assumption driven by empirical observations is that the coefficient of friction is not constant but depends on the relative sliding velocity. However, if such a dependence is taken into account there is no reason to expect that velocity and normal force will be the only parameters that affect the frictional force. Numerous models have been proposed to account for such effects, such as 'rate-and-state' models or laws based on contact temperature (see for example Sheng [5]). The difficulty associated with incorporating such a law into a model of friction-induced vibration has left the question of its importance still in debate.

Within the context of a linearised theory these models simplify and can be described within a single framework. Consider the variation of frictional force when a small oscillating tangential velocity is superimposed on a larger steady sliding velocity. Assuming that the perturbation is small enough for linear theory to be applicable, then the relationship between F' and N' can be expressed in a similar way to a transfer function from variation in sliding velocity to variation in tangential force:

$$F' \approx \varepsilon N_0 v' \tag{4}$$

where ε is the linearised velocity gradient of the frictional dependence and v' is the variation in relative sliding velocity. The full linearised expression relating variations in frictional force to variations in sliding velocity *and* normal force becomes

$$F' \approx \mu_0 N' + \mathrm{i}\omega\varepsilon N_0(v_1 + v_3) \tag{5}$$

The factor $\mathrm{i}\omega$ converts the displacements v_1 and v_3 into velocities such that $v' = \mathrm{i}\omega(v_1 + v_3)$. Note that in general, ε can be expected to be complex and frequency dependent.

Considering the transfer functions from all the inputs to all the outputs results in two characteristic functions:

$$E_1 = D + \mathrm{i}\omega\varepsilon N_0[(G_{11} + H_{11} + 1/k_n)(G_{22} + H_{22} + 1/k_t) - (G_{12} + H_{12})^2] \tag{6}$$

$$E_2(\omega) = 1 + \mathrm{i}\omega\varepsilon N_0(G_{22} + H_{22} + 1/k_t) \tag{7}$$

The system will be stable if and only if all the zeros of both $E_1(\omega)$ and $E_2(\omega)$ lie in the upper half-plane [13,16].

3. Root locus of predictions

Before looking at the convergence behaviour of predictions as more modes are included in the system model, the effect of the chosen assumptions for the contact model needs to be studied. There are several physical effects to consider: a constant coefficient of friction μ_0, contact stiffnesses k_n and k_t, and the linearised 'sliding friction transfer function' ε. The effect of varying the coefficient of friction is relatively well-understood (e.g. Hoffmann [8], Sinou and Jezequel [17]) but the effects of contact stiffness and velocity-dependence have been less systematically explored and they are therefore studied here using an example system. The system chosen for study is based on a laboratory rig which has been used for extensive experimental testing. It consists of a circular disc and a point-contact 'brake' subsystem with carefully designed dynamic characteristics to give only a small number of modes in the frequency range studied (up to 15 kHz); more details are given by Duffour and Woodhouse [18]. The transfer function matrices **G** and **H** for the two subsystems were measured using standard vibration test methods and fitted using modal analysis procedures. The fitted modal parameters used for the models throughout this paper are summarised in Table 1.

Fitting allows the transfer functions to be approximately expressed as a modal summation (e.g. Skudrzyk [19]). For example, $D(\omega)$ can be written as

$$D = \sum_{\text{all } j \text{ (disc)}} \frac{g_{u_1}^{(j)} g_{u_1}^{(j)} + \mu_0 g_{u_1}^{(j)} g_{v_1}^{(j)}}{\omega_j^2 + 2\mathrm{i}\zeta_j\omega_j\omega - \omega^2} + \sum_{\text{all } j \text{ (brake)}} \frac{h_{u_2}^{(j)} h_{u_2}^{(j)} + \mu_0 h_{u_2}^{(j)} h_{v_2}^{(j)}}{\omega_j^2 + 2\mathrm{i}\zeta_j\omega_j\omega - \omega^2} + \frac{1}{k_n} \tag{8}$$

Table 1
Uncoupled pin and disc modes sorted into sequential order by increasing frequency for the range 0–15 kHz.

Frequency range (kHz)	Frequency (Hz)	Brake mode no.	Disc mode no.	a_{11} (kg^{-1})	a_{12} (kg^{-1})	a_{22} (kg^{-1})
0–1	20	1		0.21	0.01	0.00
	193		$1^{(1,0)}$	0.67	0	0.29
	613		$2^{(0,0)}$	1.32	0	0.30
	896	2[a]		8.29	−14.37	24.92
1–5	1002		$3^{(2,0)}$	2.17	0	0.01
	2083		$4^{(3,0)}$	2.20	0	0.14
	2656	3		5.72	16.89	49.85
	3573		$5^{(4,0)}$	2.21	0	0.25
5–10	5380		$6^{(5,0)}$	2.14	0	0.37
	6327		$7^{(2,1)}$	0.41	0	0.04
	7468		$8^{(6,0)}$	2.00	0	0.52
	8698		$9^{(3,1)}$	0.15	0	0.00
	9806		$10^{(7,0)}$	1.98	0	0.58
10–15	11 154	4[a]		0.05	−2.00	73.68
	11 571		$11^{(4,1)}$	0.06	0	0.01
	12 365		$12^{(8,0)}$	1.87	0	0.90

[a] Pin modes with a negative cross term. The notation (m,n) denotes a disc mode with m nodal diameters and n nodal circles.

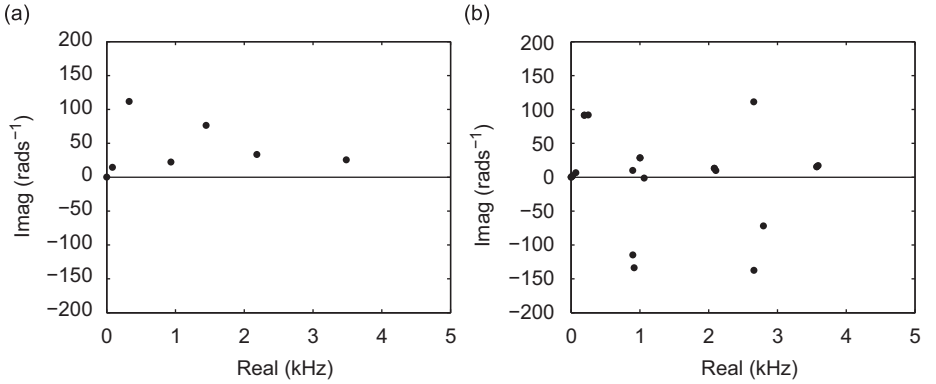

Fig. 2. Nominal predicted roots for disc rotating clockwise, using two different modelling assumptions. (a) $k_n \to \infty$, $\varepsilon = 0\,\mathrm{N\,s\,m^{-1}}$. (b) $k_n = 2\times10^6\,\mathrm{N\,m^{-1}}$, $\varepsilon = 10\,\mathrm{N\,s\,m^{-1}}$.

where ω_j and ζ_j are the natural frequency and damping factor of the jth mode, respectively, of either the disc or the brake (when the uncoupled modes of both subsystems are sorted by ascending frequency, the jth mode could correspond to either the disc or the brake). Mass-normalised modal amplitudes that correspond to the disc subsystem are denoted by g, and those for the brake h. As there is no mathematical distinction between the modal sums of the disc and the brake they can be combined. For convenience we define the modal coefficient $a_{pq}^{(j)}$ to represent the relevant product of modal amplitudes of either subsystem for the jth mode, such that we can rewrite $D(\omega)$ more compactly:

$$D = \sum_{\text{all } j} \frac{a_{11}^{(j)} + \mu_0 a_{12}^{(j)}}{\omega_j^2 + 2\mathrm{i}\zeta_j\omega_j\omega - \omega^2} + \frac{1}{k_n} \tag{9}$$

Values of a_{11} and a_{12} for the chosen system are also given in Table 1. Finding the roots requires solving the equation:

$$\sum_{\text{all } j}(a_{11}^{(j)} + \mu_0 a_{12}^{(j)}) \prod_{\text{all } k(\neq j)} (\omega_k^2 + 2\mathrm{i}\zeta_k\omega_k\omega - \omega^2) + \frac{1}{k_n}\prod_{\text{all } j}(\omega_j^2 + 2\mathrm{i}\zeta_j\omega_j\omega - \omega^2) = 0 \tag{10}$$

For any finite number of included modes, this is a polynomial. In the same way, the zeros of the characteristic functions E_1 and E_2 can also be expressed as the roots of polynomials.

Fig. 2(a) shows an example set of predicted roots (from Duffour and Woodhouse [18]) assuming the disc is rotating clockwise (μ_0 positive), neglecting contact stiffness or any velocity-dependence of friction and including all identified modes below 5 kHz. Fig. 2(b) shows the equivalent predictions using E_1 and E_2, for a model which includes both contact

stiffness (with $k_n = k_t = 2 \times 10^6$ N m) and a velocity-dependent coefficient of friction (with a constant, real value such that the product $\varepsilon N_0 = 10\,\mathrm{N\,s\,m^{-1}}$). The values chosen have been measured and are representative of actual sliding conditions in the test rig on which this model system is based: preliminary results from Wang [20] provide an order of magnitude measurement of ε for the contacting materials in our test rig (polycarbonate pin on a steel disc) giving $\varepsilon \approx 1\,\mathrm{s\,m^{-1}}$. For a typical value of the normal pre-load of 10 N the product is $\varepsilon N_0 \approx 10\,\mathrm{N\,s\,m^{-1}}$.

It is clear that the inclusion of these extra model ingredients has a significant effect which needs to be understood. This section shows the effect of varying the parameters k_n, k_t and ε and explores how predictions converge for their limiting values.

The limit in which contact stiffness $k_n \to 0$ (so that $1/k_n \to \infty$) corresponds physically to the brake and the disc becoming uncoupled. Under the simplest model the characteristic equation from $D(\omega)$ becomes

$$\sum_{n=1}^{N} a_n \prod_{p=1(\neq n)}^{N} (\omega_p^2 + 2\mathrm{i}\zeta\omega_p\omega - \omega^2) + \frac{1}{k_n}\prod_{p=1}^{N}(\omega_p^2 + 2\mathrm{i}\zeta\omega_p\omega - \omega^2) \to \frac{1}{k_n}\prod_{p=1}^{N}(\omega_p^2 + 2\mathrm{i}\zeta\omega_p\omega - \omega^2) = 0 \tag{11}$$

the solutions of which are the uncoupled poles. The same result can also be shown to be true for the characteristic functions E_1 and E_2. In the opposite limit, as $k_n \to \infty$ the solutions should converge on the solutions to the model without contact stiffness as $1/k_n \to 0$. In addition as $k_n \to \infty$ the order of the polynomial decreases by two so that two solutions must vanish.

For the case of a constant coefficient of friction, the characteristic equation for general k_n can be written as

$$1 + k_n \frac{\sum_{n=1}^{N} a_n \prod_{p=1(\neq n)}^{N} (\omega_p^2 + 2\mathrm{i}\zeta\omega_p\omega - \omega^2)}{\prod_{p=1}^{N} (\omega_p^2 + 2\mathrm{i}\zeta\omega_p\omega - \omega^2)} = 0 \tag{12}$$

This is in the standard form for obtaining the root locus diagram for a system with gain k_n. As already stated, as k_n varies from zero to infinity the roots will move from the open loop poles (the uncoupled poles) to the finite open loop zeros (the zeros of $D(\omega)$ when the contact spring becomes rigid). Using the standard root locus rules (e.g. Dorf and Bishop [21]) the remaining two roots will tend to infinity at asymptotic angles of 0° and 180° (for the complex ω-plane rather than s-plane). The imaginary part of these asymptotes is given by

$$\mathrm{Im}(\omega_z) = \frac{\sum p_i - \sum z_i}{P - Z} \tag{13}$$

where p_i are the uncoupled poles, z_i are the zeros of the simplest $D(\omega)$ and P and Z are, respectively, the numbers of poles and zeros.

Numerical tests confirm each expectation, using a model without a velocity-dependent coefficient and including all modes below 5 kHz: Fig. 3 shows the root loci of the clockwise and anticlockwise cases with the contact stiffness varying over the range $100 < k_n < 1 \times 10^{10}\,\mathrm{N\,m^{-1}}$. The uncoupled poles are shown as circles and the final roots of the characteristic function as crosses. The asymptote is superimposed as a horizontal line, and is in agreement with the loci of the highest frequency roots. Higher bandwidth tests confirm these results but are not shown here as they are less clear when plotted on one figure. Note that contact stiffness is likely to be a function of wear in addition to the normal pre-load. Therefore it will vary with time and may contribute to the difficulty in obtaining repeatable results.

When a velocity-dependent coefficient of friction is included then the root locus of E_1 as contact stiffness varies cannot be analysed in the same way as above (the root locus of E_2 is considered briefly later in this section). It is still true, however, that as $k_n \to 0$ the characteristic zeros tend to the uncoupled poles, in addition to a pole at the origin due to the factor of $\mathrm{i}\omega$, and as $k_n \to \infty$ they converge on the characteristic zeros of the model with a velocity-dependent coefficient of friction but no contact stiffness. As it is expected that k_n and k_t are of a similar order of magnitude they are taken to be equal in the

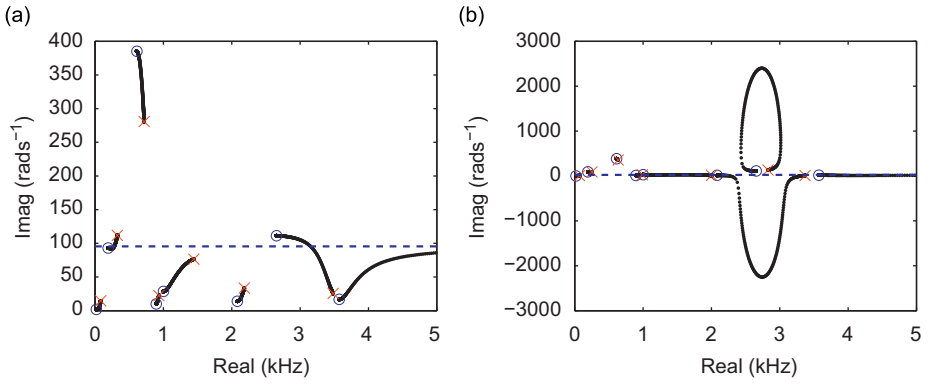

Fig. 3. Root loci as k_n varies. Uncoupled poles (circles), final coupled zeros (crosses), and asymptote of vanishing root (dashed line) superimposed. Model does not include velocity-dependent coefficient of friction. (a) Clockwise. (b) Anticlockwise.

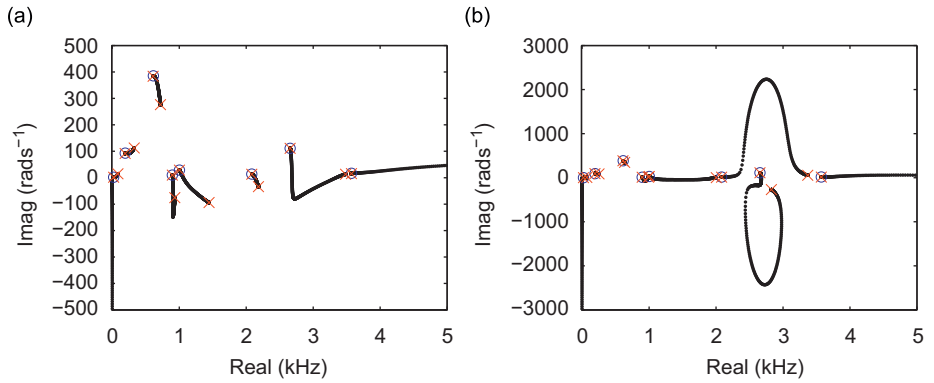

Fig. 4. Root loci as k_n varies. Uncoupled poles (circles) and final coupled zeros (crosses) superimposed. Model includes velocity-dependent coefficient of friction. (a) Clockwise. (b) Anticlockwise.

following analysis. Three roots must vanish but their asymptotes cannot be immediately intuited as the problem cannot be expressed in standard root locus form.

Numerical results are shown in Fig. 4 for $\varepsilon N_0 = 10\,\mathrm{N\,s\,m^{-1}}$. It can be seen that two roots tend to infinity at angles of 0° and 180° and the remaining root tends to minus infinity along the imaginary axis from the origin (this is less clear in (a) but viewing a wider bandwidth confirms this). It appears that a coupled root is coincident with each uncoupled pole: although not visible on the plot closer inspection reveals that they are distinct, and that two locus segments stem from each uncoupled pole. One of these is very short and ends on the almost coincident coupled root while the others form the visible segments. It is expected that two segments begin from every uncoupled pole as the inclusion of ε approximately doubles the polynomial order. The observation that half of the segments are so short shows that the extra set of coupled roots are close to the uncoupled poles, indicating that this value of εN_0 is small for this system. This is made apparent by considering the limiting values of ε.

The term ε always appears in the product εN_0 so these terms will be considered together. As $\varepsilon N_0 \to 0$ then approximately half of the roots will converge on the case without a velocity-dependent coefficient (the roots of $D(\omega)$) and the other half on the uncoupled poles which in the limit become pole-zero cancellations. As $\varepsilon N_0 \to \infty$ the roots will converge on the zeros of $\det(\mathbf{G}+\mathbf{H})$. The characteristic function E_1 can be written in standard root locus form

$$1 + \varepsilon N_0 \frac{\mathrm{i}\omega \det(\mathbf{G}+\mathbf{H})}{D(\omega)} = 0 \tag{14}$$

so any asymptotes of the remaining roots will follow the usual rules. The difference between the number of poles and zeros is one (whether or not contact stiffness is included), and so the asymptote should tend to infinity as $\varepsilon N_0 \to 0$ at an angle of -90° starting from the origin. To retain conjugate symmetry this must be along the imaginary axis. Fig. 5 confirms this with εN_0 varying from 1×10^{-4} to $1 \times 10^{4}\,\mathrm{N\,s\,m^{-1}}$. The circles and crosses still represent the uncoupled poles and simple coupled roots (from $D(\omega)$) and both now correspond to $\varepsilon N_0 \to 0$. The roots of $\det(\mathbf{G}+\mathbf{H})$ are not shown as these have no obvious intuitive meaning. Higher bandwidths have also been tested and convergence can be demonstrated in each case except in the region near 10 kHz where numerical sensitivity is a limiting factor.

The characteristic function E_2 can be expressed in standard form whether k_t or εN_0 is varied and the root loci in each case begin or end at the uncoupled poles. When varying εN_0 the other extreme of the loci are the roots of $G_{22} + H_{22} + 1/k_t$ and when varying k_t the other extreme is at the roots of E_2 in the absence of k_t. In each case an asymptote occurs along the negative imaginary axis. The details of the loci in each of these cases do not provide any further insight and have not been shown here.

4. Validity of using a reduced set of modes

We now focus on the convergence behaviour as different numbers of modes are included in the model using representative values of k_n, k_t and ε. It is expected that a model which includes all identified uncoupled modes over the measured bandwidth should provide the most accurate prediction of the coupled behaviour: such a model will be referred to from now as a 'global' model although strictly it is still a 'local' description of the true system dynamics. A natural question to ask is: What is the smallest number of modes required to give a 'reasonable' approximation to the global prediction?

Much of the literature suggests that two modes are often sufficient, assuming a 'mode-coupling' route to instability (e.g. Nack [22], Hoffmann [8], Huang [23]). In the simplest case, two undamped modes are included in a model. As a parameter (e.g. the coefficient of friction) is varied, the roots of the characteristic function are either marginally stable or a symmetric pair: one stable and the other unstable. Therefore the limit of stability occurs when the two roots coincide, hence the term

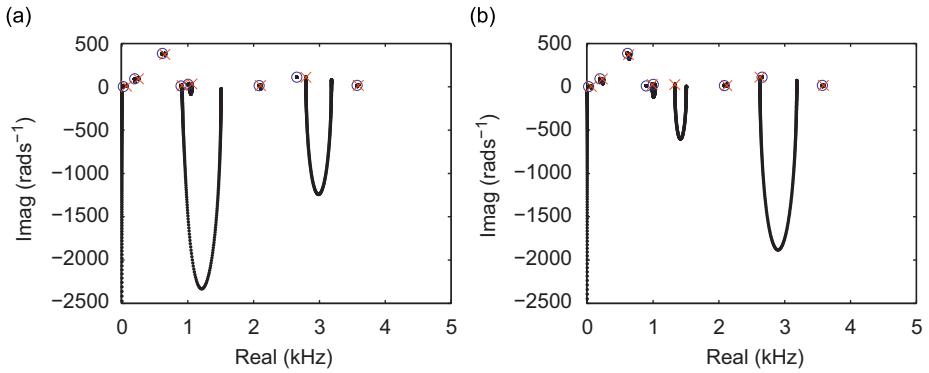

Fig. 5. Root loci as εN_0 varies. Uncoupled poles (circles) and final coupled zeros (crosses) superimposed. Model includes contact stiffness. (a) Clockwise. (b) Anticlockwise.

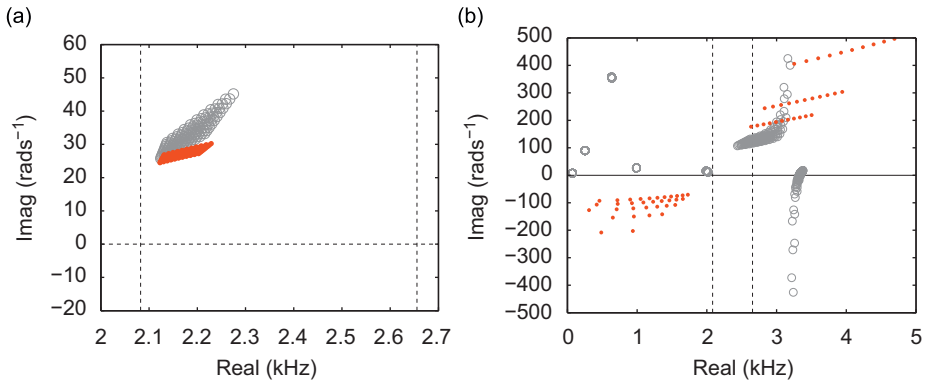

Fig. 6. Two-mode local approximation of global system: (dots) local prediction, (circles) global prediction. Local model consists of pin mode 3 and disc mode 4. (a) Clockwise. (b) Anticlockwise.

'mode-coupling'. It is recognised that in the presence of damping this is more complicated and the threshold of stability is no longer at the coincidence of the roots (e.g. Hoffmann [24], Fritz et al. [25]), but it is hypothesised that this is the essential mechanism that leads to many occurrences of squeal. Giannini and Sestieri [26] also discuss the mode-coupling route to instability but draw a subtle distinction. Here the modes included in the model are a brake mode and a disc mode that are close in frequency. However, both polarisations of the disc mode are included so this is strictly a three-mode model and the authors discuss the complicated interaction of the roots as the modal parameters vary. Duffour and Woodhouse [16] also suggested that three modes may provide a minimal model as this is the simplest case for which instabilities can be predicted within the bandwidth of the uncoupled poles using a model that neglects both contact stiffness and a velocity-dependent coefficient of friction.

4.1. Constant coefficient of friction

It is difficult to conclude how well a reduced system approximates the full system if just the nominal roots of both models are compared: the two can only be said to be in agreement in a sense useful for design calculations if the effect of perturbations is also similar in trend for both systems. Therefore, in the following investigations, two relevant parameters are varied about their nominal measured values and the resulting clouds of predictions compared between models.

Beginning with the simplest model with infinite contact stiffness and neglecting any velocity-dependence of the coefficient of friction, the predictions near the third pin mode at 2.6 kHz will be considered. If just this third mode is included in the model then no solutions to the characteristic polynomial exist. For this simple model a minimum of two modes must be included. This results in a symmetric pair of solutions with positive and negative frequencies and therefore one positive frequency root prediction.

Fig. 6 shows a comparison of this local model (dots) with the global model (circles). The most optimistic bandwidth of validity is shown by vertical dashed lines and is simply defined by the minimum and maximum frequencies included in the local model. The natural frequency of the third pin mode is varied by ± 10 percent and the coefficient of friction between 0.4 and 0.6 in each of the clockwise and anticlockwise directions. It can be seen that the stable prediction in (a) is rather well approximated with similar trends in the root locations as the parameters vary. Note that no instability can be

predicted by this two-mode model within the bandwidth of the uncoupled poles. The local predictions in (b) are poor approximations of the global prediction, but perhaps this is not too surprising as virtually all the local predictions lie outside of the expected bandwidth of validity. Instability in this case is predicted outside this bandwidth (as is possible for this model).

Including the fifth disc mode forms a cluster of three modes centred on the third pin mode (refer to Table 1). As for the two-mode case the local predictions for the clockwise direction are stable and approximate the global predictions rather well (not shown). However, the anticlockwise local predictions are completely different, and much more sensitive than the global predictions. The results continue to follow this pattern when the third and sixth disc modes are successively added. Only upon inclusion of the second pin mode is convergence reached for the anticlockwise predictions. Fig. 7(a) shows this six-mode local prediction compared with the global model and it can be seen that there is now excellent agreement. The importance of including this second pin mode, and the relatively insignificant effect of the disc modes included so far, suggests a further test. Fig. 7(b) shows the two-mode local predictions using just the second and third pin modes. There is still a surprisingly good level of agreement, although the clockwise local predictions for this case are less good (not shown). The minimal model to give a reasonable local approximation to the global system (over a bandwidth of validity that includes the third pin mode) turns out to require the second and third pin modes with the third and fourth disc modes (not shown).

It may seem unsurprising that both pin modes must be included in the model as the amplitude of their modal coefficients are an order of magnitude greater than those of the disc. Perhaps more unexpected is that the two most important modes are neither particularly close in frequency nor consecutive modes of the system. In addition, for reasonable predictions in both directions the small amplitude disc modes needed to be included. Note that by 'amplitude' of a mode the intended meaning is its contribution to the uncoupled transfer function at the contact.

In a similar way, it turns out that in order to make an approximate prediction of the instability near 3.5 kHz in the anticlockwise direction the minimal model requires the second and third pin modes with the fifth disc mode (see Fig. 8(a)). A model that includes the third pin mode with the fifth and sixth disc modes is a much poorer approximation to the global system as shown in Fig. 8(b). The approximation remains poor in this frequency band even if every other mode is included

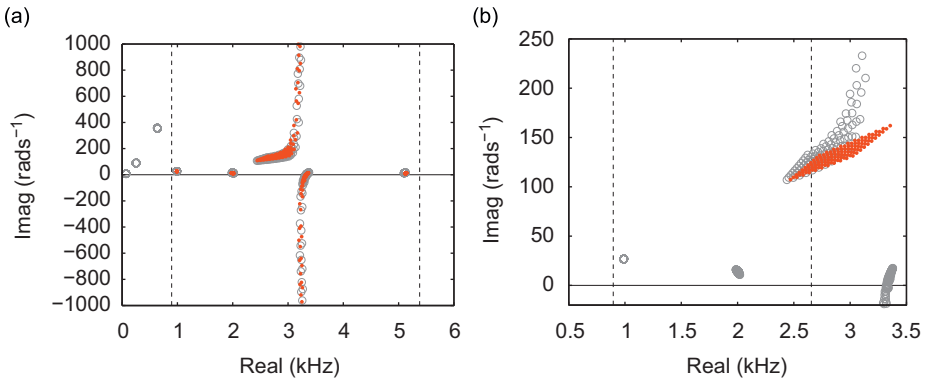

Fig. 7. Effect of including pin mode 2—local approximations of global system: (dots) local prediction, (circles) global prediction. Local model consists of (a) pin modes 2 and 3 and disc modes 3–6, (b) pin modes 2 and 3.

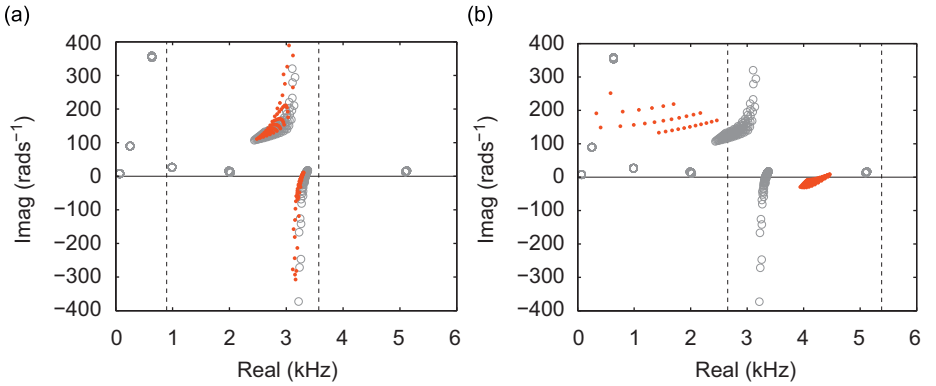

Fig. 8. Three-mode models highlighting importance of pin mode 2 for anticlockwise predictions—local approximations of global system: (dots) local prediction, (circles) global prediction. (a) Pin: 2, 3/disc: 5. (b) Pin: 3/disc: 5, 6.

except for the second pin mode, though the approximation becomes better at higher frequencies. It is interesting that a single mode could be so important, suggesting that including sufficient bandwidth alone cannot guarantee convergence. This raises the possibility that a mode outside of the measured frequency range could make a significant difference to predictions, but the convergence of the previous case at higher frequencies suggests such an effect might only be expected towards the limiting frequencies of the model. It is also interesting that the fifth disc mode is necessary to predict this instability, suggesting that the amplitude of modal coefficients alone does not determine the effect on predictions. This question is discussed further in Sections 6 and 7.

4.2. Contact stiffness

The inclusion of contact stiffness allows the consideration of a single-mode local model (see Butlin and Woodhouse [13]). The value for the contact stiffness chosen for the subsequent tests is $k_n = 2 \times 10^6\,\mathrm{N\,m^{-1}}$ (obtained from measurements on the test rig described by Duffour and Woodhouse [18]), unless otherwise stated. Fig. 9 shows an example single-mode model that includes just the third pin mode for predictions in both directions. The bandwidth of validity in this case is a single line, and predictions would only be expected to be good approximations close to this. The agreement is surprisingly good and predictions using the single-mode model for each uncoupled mode in both directions are consistently good approximations of the corresponding roots of the global prediction. However, it should be noted that there is no instability or region of high sensitivity predicted by either the global or local models.

Using lower values for contact stiffness gives progressively improved agreement between local and global models. However, the predictions diverge for higher values of the contact stiffness. Fig. 10 shows the clockwise and anticlockwise predictions for $k_n = 4 \times 10^6\,\mathrm{N\,m^{-1}}$. It can be seen that the clockwise prediction is still a good approximation but that the anticlockwise predictions are beginning to diverge. This seems to be due to the instability predicted in the global model: single-mode predictions with contact stiffness can only be unstable if the real part of the root is zero (see Butlin and Woodhouse [13]). Therefore as soon as a multi-degree of freedom model predicts instability, the single-mode model automatically becomes a poor approximation. For this higher value of contact stiffness the model improves by simply including the nearest mode: in this case the fourth disc mode (see Fig. 11). Nevertheless the improvement is limited: the

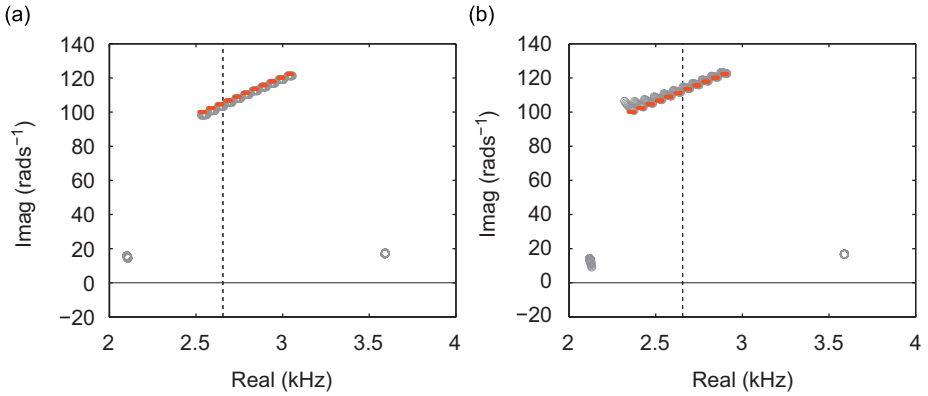

Fig. 9. Single-mode local approximation of global system: (dots) local prediction, (circles) global prediction. Local model consists of pin mode 3 with $k_n = 2 \times 10^6\,\mathrm{N\,m^{-1}}$. (a) Clockwise. (b) Anticlockwise.

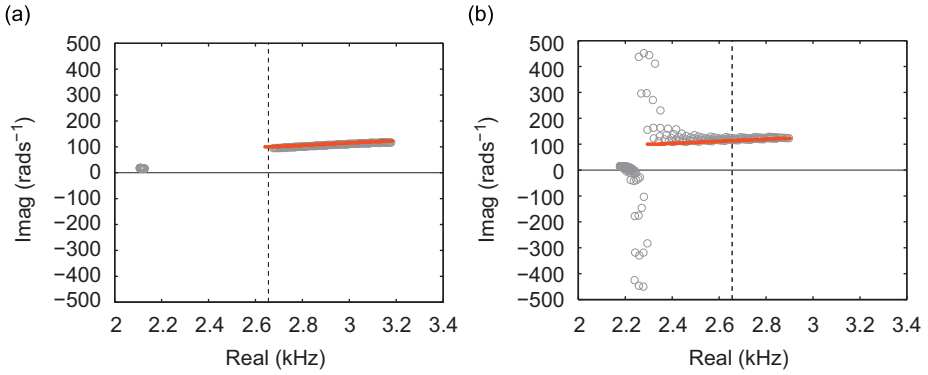

Fig. 10. Single-mode local approximation of global system: (dots) local prediction, (circles) global prediction. Local model consists of pin mode 3 with $k_n = 4 \times 10^6\,\mathrm{N\,m^{-1}}$. (a) Clockwise. (b) Anticlockwise.

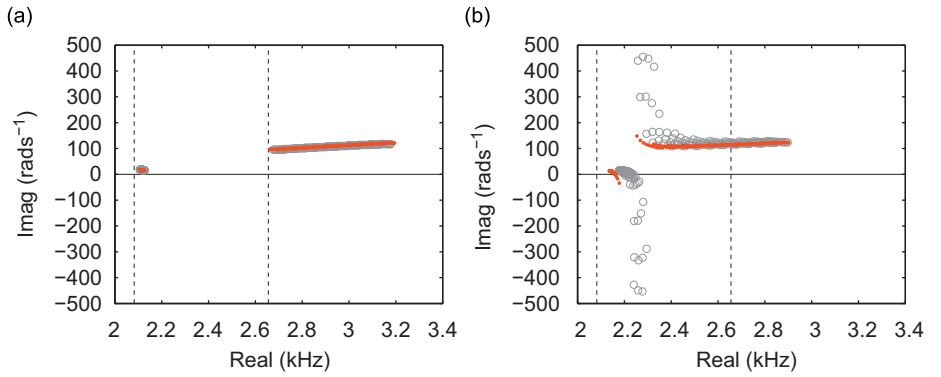

Fig. 11. Two-mode local approximation of global system: (dots) local prediction, (circles) global prediction. Local model consists of pin mode 3 and disc mode 4 with $k_n = 4 \times 10^6\,\mathrm{N\,m^{-1}}$. (a) Clockwise. (b) Anticlockwise.

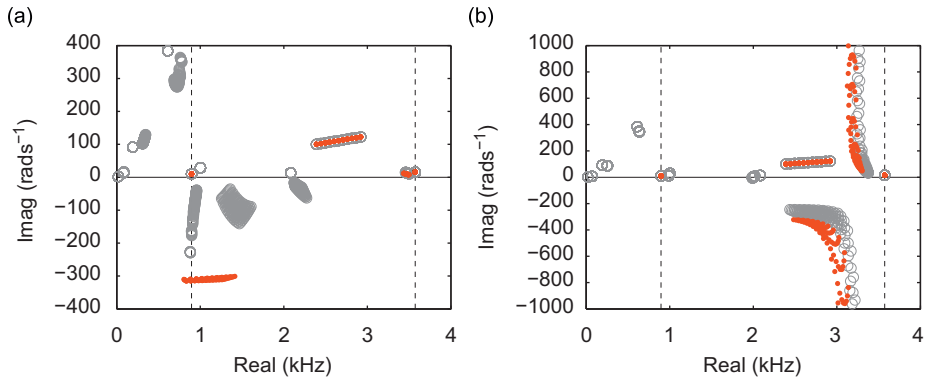

Fig. 12. Three-mode minimal model—local approximations of global system: (dots) local prediction, (circles) global prediction. Local model consists of pin modes 2 and 3 and disc mode 5 with $\varepsilon N_0 = 10\,\mathrm{N\,s\,m^{-1}}$. (a) Clockwise. (b) Anticlockwise.

instability is only just predicted and the sensitivity is underestimated. Inclusion of the fifth disc mode also results in reasonable agreement but is less useful as the bandwidth of validity does not include the instability. In the previous section it was seen that the second pin mode was extremely important and if included in this model, it also improves the predictions enormously.

4.3. *Velocity-dependent coefficient of friction*

A single-mode model that includes a velocity-dependent coefficient of friction but infinite contact stiffness leads to the characteristic function E_1 reducing to D which has no solutions (see Butlin and Woodhouse [13]). A single-mode model can therefore never be a good approximation to the global system in this case. Testing minimal models using $\varepsilon N_0 = 10\,\mathrm{N\,s\,m^{-1}}$ in the region of the third pin mode results in anticlockwise predictions only converging when the second pin mode is included. Fig. 12 shows the predictions from this minimal model which includes the second and third pin modes and the fifth disc mode. The convergence behaviour is similar to the local models without contact stiffness or a velocity-dependent coefficient of friction (see Fig. 8(a)). The discrepancies in the clockwise direction in (a) converge towards the global predictions if the third and fourth disc modes are also included (not shown).

Including a finite contact stiffness together with the velocity-dependent friction term ($\varepsilon N_0 = 10\,\mathrm{N\,s\,m^{-1}}$) gives slightly different convergence behaviour in the frequency band surrounding the third pin mode. The single-mode approximation in this case is reasonable in both directions (illustrated in Fig. 13) and including the second pin mode does not make the step change it did for the previous cases considered. However, the single-mode models are fundamentally limited, as the order of the characteristic polynomial of each model is three for both E_1 and E_2. For an N-mode global system a model that includes both contact stiffness and a velocity-dependent coefficient of friction has $4N+1$ and $2N+1$ solutions for E_1 and E_2, respectively (see Butlin and Woodhouse [13]). Therefore N single-mode models cannot make predictions that correspond to every solution of E_1 and would make too many predictions for a one-to-one correlation with E_2.

Two-mode models using pairs of poles can often provide reasonable local approximations to the global prediction, but these can sometimes be strongly affected by a nearby third mode and also frequently miss features of the global predictions

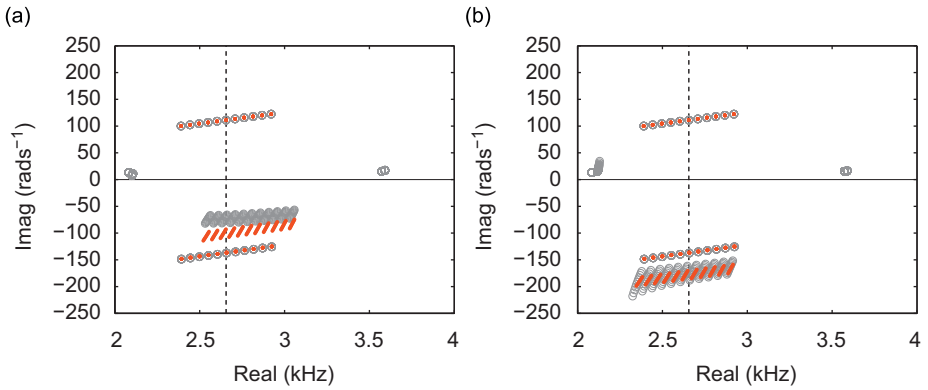

Fig. 13. Single-mode model including contact stiffness and velocity-dependent coefficient of friction ($\varepsilon N_0 = 10\,\mathrm{N\,s\,m^{-1}}$)—local approximations of global system: (dots) local prediction, (circles) global prediction. Local model consists of pin mode 3. (a) Clockwise. (b) Anticlockwise.

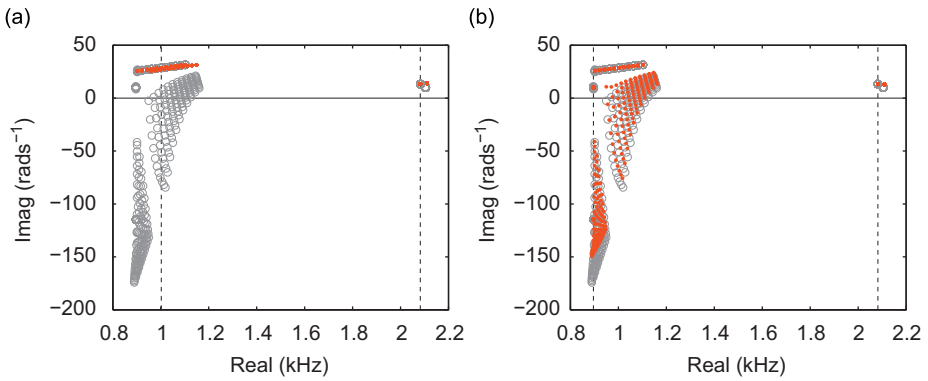

Fig. 14. Two- and three-mode models—local approximations of global system: (dots) local prediction, (circles) global prediction. Model includes velocity-dependent coefficient of friction and contact stiffness. (a) Disc modes: 3, 4. (b) Pin mode: 2/disc mode: 3, 4.

within the intended bandwidth of validity (illustrated in Fig. 14 with the frequency of the third disc mode varied by 10 percent). It seems that usually a set of three modes can be chosen to well approximate most global predictions over their bandwidth but some of the cases discussed above have shown that these are not always consecutive modes and may sometimes be surprisingly remote in frequency.

5. Validity of three-mode approximation

The following analysis considers more closely the validity of three-mode local models that use uncoupled modes selected consecutively. Fig. 15 shows all the predictions that are within the bandwidth of validity from each consecutive three-mode model, superimposed on the global predictions. For each three-mode model the natural frequency of the first disc mode in the sequence was varied by 10 percent. The same mode in the global model was also varied by the same amount. The resulting predictions for each local model has been truncated to the expected bandwidth of validity.

Some of the roots are in good agreement and closer inspection of the low frequency clusters shows that the trends are very similar even if the root locations differ. It is clear though that some of the three-mode predictions are insufficient to approximate the global system, for example the instability near 3.6 kHz in the anticlockwise direction is not predicted. This has already been seen to require a combination of the second and third pin modes in the local model.

Applying the same strategy to a model that includes contact stiffness (with $k_n = 2 \times 10^6$) gives remarkably good agreement across the bandwidth of the global model (not shown). In this case the global model predictions are all stable and fairly insensitive to perturbations. It was noted in Section 4.2 that low-order models gave an accurate local approximation for values of the contact stiffness that were relatively low, where $k_n \approx 4 \times 10^6\,\mathrm{N\,m^{-1}}$ seemed to mark the threshold. This is consistent with the discrepancies observed above without contact stiffness where $k_n \to \infty$. It also seems that agreement is better for the stable (and insensitive) roots. But such agreement is of limited value when instability and sensitivity are of most interest.

Adding a velocity-dependent coefficient of friction to the model (with $\varepsilon N_0 = 10\,\mathrm{s\,m^{-1}}$) gives similarly good agreement between local and global predictions below 8 kHz (see Fig. 16). Above this frequency the mean of the groups seems to be

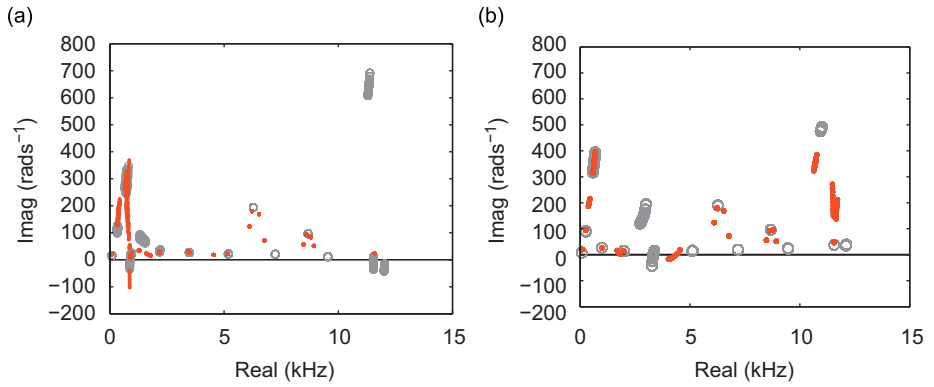

Fig. 15. Consecutive three-mode models superimposed—local approximations of global system: (dots) local prediction, (circles) global prediction. Model has infinite contact stiffness and no velocity dependent coefficient of friction. (a) Clockwise. (b) Anticlockwise.

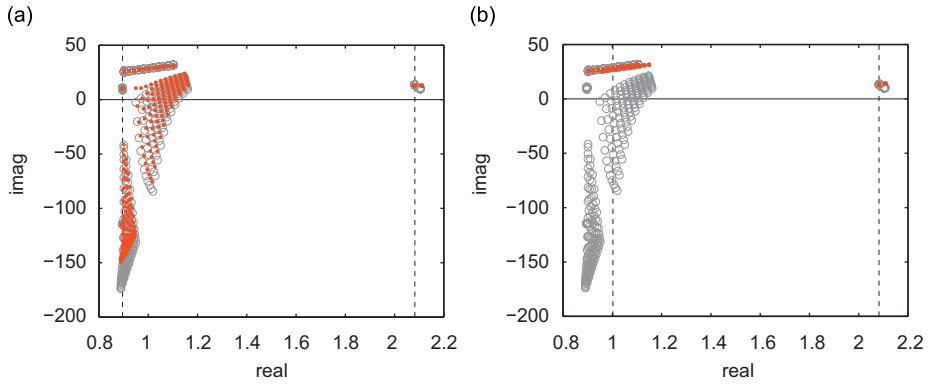

Fig. 16. Consecutive three-mode models superimposed—local approximations of global system: (dots) local prediction, (circles) global prediction. Model includes finite contact stiffness and a velocity-dependent coefficient of friction. (a) Clockwise. (b) Anticlockwise.

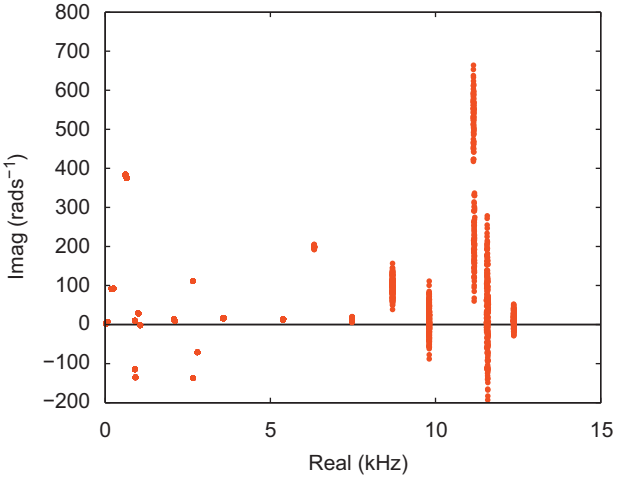

Fig. 17. Roots of global characteristic polynomial whose coefficients have been randomly perturbed by the limit of finite precision 100 times. Model includes finite contact stiffness and a velocity-dependent coefficient of friction.

well approximated but there is significantly greater sensitivity in the global predictions. This is largely a result of numerical sensitivity: Fig. 17 shows the roots of a nominal characteristic polynomial whose coefficients have been randomly perturbed by the limit of finite precision and solved 100 times (the results shown are for clockwise disc rotation only as the anticlockwise results are very similar).

It is interesting that the very small polynomial perturbations should have an effect on the predictions that is similar in magnitude to much larger parameter perturbations. One possibility is that this uncertainty is a purely numerical artefact. Changing a parameter causes a structured perturbation to the coefficients of the characteristic polynomial: the solution of the polynomial may be robust to this structured change, but highly sensitive to individual coefficient perturbations. If the structured perturbation is imperfectly represented by finite precision arithmetic, its effect is similar to introducing random coefficient perturbations. This would result in similar uncertainties resulting from both kinds of perturbation, as is observed.

Another possibility is that the physical system is extremely sensitive to parameter perturbations, but highly nonlinearly, so that a small perturbation causes a similar change in predictions to a larger perturbation.

Several tests have been carried out which support the first possibility. A first-order perturbation analysis (details can be found in Butlin [15]) also results in prediction uncertainties of a similar order of magnitude for both perturbation types. Had the sensitivity been physical, the uncertainties resulting from parameter perturbations might have been expected to have been proportionally greater than those resulting from coefficient perturbations as any limiting nonlinearities are ignored in the first-order analysis. In addition, increasing the amplitude of the random coefficient perturbations significantly increased the resulting uncertainties beyond that of the parametric uncertainties. Therefore it is possible that the local three-mode models may be providing a more accurate description of the true coupled system behaviour at high frequencies if the numerical sensitivity is not masking true parametric sensitivity.

While the models with finite contact stiffness or a velocity-dependent coefficient of friction (Fig. 16) suggest that three consecutive modes are sufficient for a minimal local model, the case without either (Fig. 15) flags a warning that this cannot be universally true for all values of εN_0 and k_n as it represents the limiting case of these variables. Therefore it is worth considering what other factors are significant for determining a valid reduced-order model.

6. Significance of small amplitude modes

It may be expected that three-mode models would only be valid if describing an isolated tight cluster of modes. However, the importance of the combination of the second and third pin modes in some of the models described above seems to contradict this. It may simply be that there is no cluster of three modes isolated enough within the global model for such a three-mode model to be valid, but if this is the case then the concept of an isolated cluster loses its value in practical terms where isolated groups of three modes would be rare. In addition, it does not seem to be a case of simply requiring more modes within a model, as a three-mode system can usually be found that does give a good approximation, but not necessarily based on consecutive modes.

It is of interest to consider what are the key elements of a model in order to find more reliable methods of reducing the order of a global model to create a minimal local model for a particular bandwidth of interest. There are several motivations for reducing the model order: to confirm the validity of global predictions; to understand the key factors governing coupled root locations; and to provide a way of simplifying ill-conditioned problems without discarding key properties of the system that govern stability and sensitivity.

A natural option to explore is to neglect small amplitude modes. A systematic sequence of simulations to test this idea is briefly described here. Of course, the definition of a 'small amplitude mode' is not entirely clear-cut. A driving-point modal coefficient of a given mode may be large while the cross-coupling term may be very small. The model choice also matters: if a velocity-dependent coefficient of friction is included then the tangential driving point terms (G_{22} and H_{22}) come into play, but are irrelevant if not.

The strategy adopted for the tests was first to limit the bandwidth to the broad frequency range of interest, then remove terms in ascending order of amplitude such that driving point terms in the normal and tangential directions were assessed for deletion independently. Once identified, the cross-term of the same mode was also deleted (to maintain the relationship $a_{11}a_{22} = a_{12}^2$).

The level of agreement between these three-mode local models and the global models varied rather widely. While some predictions gave good agreement, cases where the global model predicted instability or sensitivity (or both) were often missed entirely. This does not allow much confidence to be placed in three-mode local models chosen either on the basis of proximity in frequency or amplitude of the modal coefficients.

7. Automated mode selection

The next logical step in identifying a mode-selection criterion that can identify reliable reduced-order models is one that takes into account both modal amplitudes and proximity to the frequency range of interest. One natural strategy is to identify a measure of the significance of each uncoupled pole for a given frequency, then select the most significant modes.

For a model that neglects a velocity-dependent coefficient of friction, the significance measure for the nth pole, $S_D^{(n)}$, found to be most effective was

$$S_D^{(n)} = \left| \frac{a_{11}^{(n)} + \mu_0 a_{12}^{(n)}}{\omega_n^2 - \omega_c^2} \right| \tag{15}$$

where ω_c is the chosen frequency of interest. This is perhaps an obvious choice (at least in retrospect), as it is simply the contribution of the nth mode to the characteristic function $D(\omega)$ (Eq. (3)) evaluated at the frequency of interest, neglecting damping. Including damping would yield the following measure:

$$S_{D\,\mathrm{alt}}^{(n)} = \left| \frac{a_{11}^{(n)} + \mu_0 a_{12}^{(n)}}{\omega_n^2 + 2\mathrm{i}\zeta_n \omega_n \omega_c - \omega_c^2} \right| \tag{16}$$

which results in negligible differences so the first measure is used for the following tests to retain simplicity.

For a given frequency of interest, ω_c, the relative significance of each mode can be determined according to the measure $S_D^{(n)}$. Modes with significance above a certain threshold could then be kept, but this was not found to be a particularly robust strategy. Instead, the three most significant modes were kept. Nevertheless this still leaves the possibility of neglecting a mode that is almost as significant as the others simply because of the specific choice of frequency. This choice is fairly arbitrary, so for more reliable model reduction, $S_D^{(n)}$ is evaluated for a range of frequencies (± 10 percent) and the highest ranking three modes for each evaluation are accumulated. Therefore this method results in models with a minimum of three modes, but where the significance measure is sensitive to the exact frequency of interest it includes additional modes that are significant. The choice of three modes is arbitrary, but was found to be an effective balance between giving significant model reduction and reliable predictions. Choosing to keep just one or two of the most significant modes produced models that often missed instabilities and sensitivities.

The strategy is now applied to the instability predicted by the global model near 3 kHz with the disc rotating anticlockwise. The automatically selected modes were pin modes 2 and 3, and disc modes 4 and 5. Fig. 18(a) shows the comparison between the local and global model predictions. The mode selection procedure has identified the importance of the second pin mode and the agreement is very good, capturing both the instability and sensitivity. For the disc rotating clockwise, the modes chosen are pin mode 3 and disc modes 4 and 5, for which the agreement is similarly good (not shown). Note that for this direction of rotation the second pin mode is correctly identified as being no longer significant.

Choosing a frequency of 1 kHz and clockwise disc rotation, the reduced-order model identified consists of pin modes 2 and 3, and disc modes 2 and 3. The comparison is shown in Fig. 18(b). The local model again captures the global model prediction of instability and sensitivity.

Taking the frequency of interest to be 11 kHz for clockwise disc rotation, pin modes 3 and 4 with disc modes 8, 10, 11 and 12 are identified for the reduced-order model. The comparison between local and global models is shown in Fig. 19. It may be thought that this does not constitute a particularly 'minimal' model and is bound to give a good approximation simply because of the number of nearby modes included. However, further tests have shown that only upon inclusion of the third pin mode, at a surprisingly remote frequency of 2.6 kHz, is reasonable agreement achieved. In addition, inclusion of any one of the neglected modes only improves the local model predictions slightly, but exclusion of any one of the selected modes more significantly worsens agreement.

The model reduction strategy has been applied to a wide range of test cases. For models that neglect a velocity dependent coefficient of friction (but may include finite contact stiffness) the reduced-order models give consistently good approximations to the global model.

It is interesting to consider the set of reduced-order models as a function of chosen frequency. This is shown in Fig. 20(a) for the disc rotating clockwise and (b) for the anticlockwise case. As expected, the reduced set of modes usually consists of those nearest in frequency. But the importance of the third pin mode for clockwise predictions and the second pin mode for anticlockwise predictions becomes very clear: their significance persists across almost the whole frequency range considered. An intuitive interpretation may be that both of these modes have relatively high amplitudes and are also strongly asymmetric (high amplitude cross-terms). They have opposite signs, so depending on the direction of rotation (hence sign of μ_0), one or other becomes particularly significant. That their importance persists across almost the whole

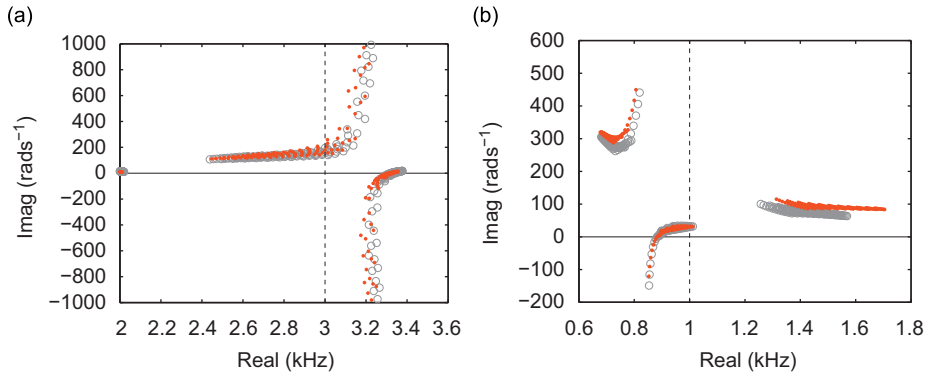

Fig. 18. Automated model reduction—local approximations of global system: (dots) local prediction, (circles) global prediction. Model assumes infinite contact stiffness and neglects a velocity-dependent coefficient of friction. (a) Clockwise. (b) Anticlockwise.

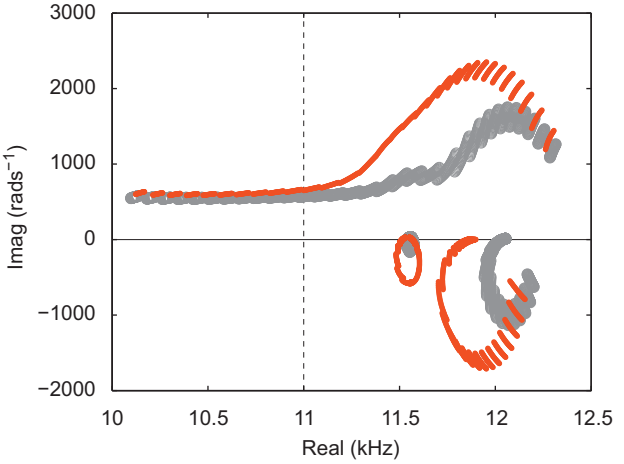

Fig. 19. Automated model reduction—local approximations of global system: (dots) local prediction, (circles) global prediction. Model assumes infinite contact stiffness and neglects a velocity-dependent coefficient of friction.

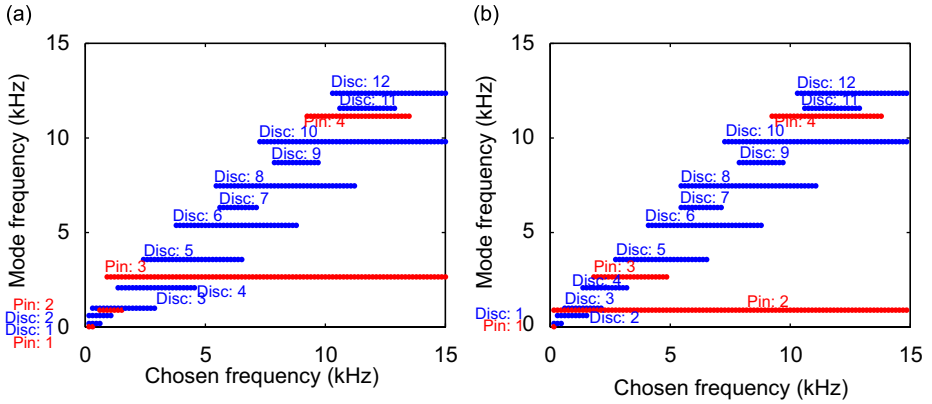

Fig. 20. Automated model reduction—selected modes as a function of frequency. (a) Clockwise. (b) Anticlockwise.

frequency range seems to be because the amplitudes of $a_{11}+\mu_0 a_{12}$ are an order of magnitude greater than for the other modes, which is enough to outweigh the $1/(\omega_n^2-\omega_c^2)$ relative reduction of significance with frequency difference.

Fig. 20 may also give some indication of prediction sensitivity to model changes. Where many modes are selected for a reduced-order model, the implication is that they are all of comparable significance, resulting in slow convergence as the number of modes is increased.

Including a velocity-dependent friction term would seem to result in a more complicated picture. If the same idea as above is applied here, then the significance measures should be the magnitude of contribution of a given mode to the characteristic functions E_1 and E_2 (Eqs. (6) and (7)). In the case of E_1 the issue is not so simple because it involves a nonlinear combination of modal contributions. One possible choice is

$$S_{E1}^{(n)}=\left|\left[\frac{a_{11}+\mu_0 a_{12}}{\omega_n^2-\omega_c^2}\right]+\mathrm{i}\omega\varepsilon N_0\left[\frac{a_{11}a_{22}-a_{12}^2}{(\omega_n^2-\omega_c^2)^2}\right]\right| \tag{17}$$

where the superscript notation that identifies each modal coefficient as the nth mode has been dropped for clarity. However, the second term in square brackets is zero because $a_{11}a_{22}=a_{12}^2$ (for proportionally damped systems with real-valued modal coefficients). It is only when terms from different modes are cross-multiplied that they contribute to this part of E_1. This leaves the first term in Eq. (17), which is the previous measure $S_D^{(n)}$, so it seems a logical starting point to use this again to identify the reduced set of modes used to solve E_1.

To choose the reduced set of modes used to solve E_2, a natural choice for the sensitivity measure is

$$S_{E2}^{(n)}=\left|\frac{a_{22}}{\omega_n^2-\omega_c^2}\right| \tag{18}$$

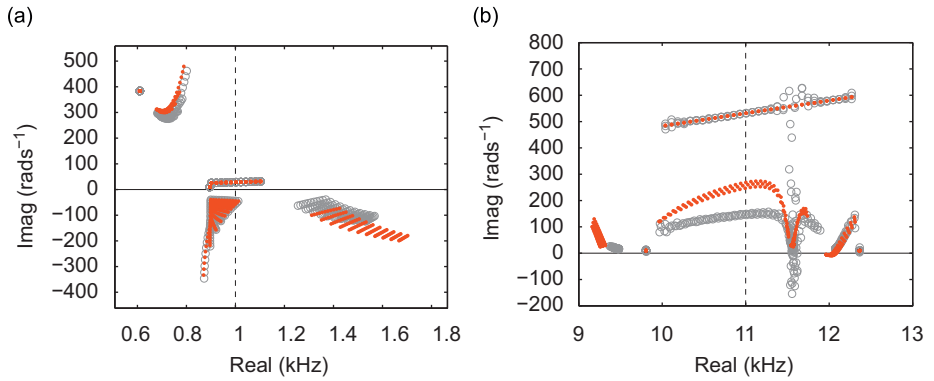

Fig. 21. Automated model reduction—local approximations of global system: (dots) local prediction, (circles) global prediction. Model assumes infinite contact stiffness but includes a velocity-dependent coefficient of friction. (a) Clockwise, 1 kHz. (b) Anticlockwise, 11 kHz.

A systematic sequence of tests has shown that in practice, simply using the original measure of significance for both characteristic functions E_1 and E_2 continues to give effective choices of modes for reduced-order models. A low and high frequency example for E_1 alone is shown in Figs. 21(a) and (b), respectively, for a model that includes a velocity dependent coefficient of friction, but infinite contact stiffness. The results for E_2 are not shown, but give very good agreement for all frequencies tested. Note that the modes chosen are the same as for the equivalent cases shown previously, as shown in Fig. 20. The low frequency local model gives excellent agreement to the global predictions. The high frequency local model represents the case where least agreement was seen. Nevertheless key features are still apparent. It seems that the sensitivity and instability near 11.5 kHz is missed by the local model, but further tests indicate that this is numerical sensitivity.

Including finite contact stiffness results in very highly sensitive predictions at high frequencies (as seen in Section 5). The low frequency local models continue to provide excellent approximations to the global model predictions. For higher frequencies the local model gives more robust predictions than the global model. As discussed previously, this may be a more reliable description of the true behaviour at high frequencies.

The robustness of the automatic model-reduction strategy to different modelling assumptions suggests the possibility of more general applicability. Although the present model is limited to the general class of sliding point-contact systems, the mechanisms identified that lead to instability will form a subclass of routes to instability of more general area contacts. Therefore it seems plausible that the equivalent modal properties of caliper and disc could be used to identify the modes most significant to a frequency of interest.

8. Conclusions

Much of the literature on friction-induced vibration focusses on reduced-order models, but previous work has shown that these can be highly sensitive to parameter and modelling details under certain conditions. The aim of reduced-order models is to approximate over a limited bandwidth the complete system behaviour. All models are in some sense reduced-order as they cannot reliably describe an infinite bandwidth, so for a model to be useful it should converge as its bandwidth of validity is increased. Conversely, if such convergence exists then it should be possible to identify a minimal model that adequately describes a local bandwidth. This paper has explored how the predictions converge as the model complexity is increased, beginning with the limiting one-, two- and three-mode models. In addition, the effect of contact stiffness and a velocity-dependent coefficient of friction upon the convergence behaviour was explored.

Limiting values of contact stiffness and the linearised velocity gradient of the coefficient of friction were tested numerically by generating root locus plots. The expected initial and final locations of the roots were compared with the numerical results and gave good agreement and convergence. In addition to validating numerical calculations of predictions, these tests provide insight into how the behaviour of sliding coupled systems evolve. In particular it is expected that as the brake wears, the contact stiffness will gradually change. Consequently the coupled root locations will vary along the corresponding root locus.

It was shown that one- and two-mode models often provided a good approximation to global models as long as the global model predictions were stable and relatively insensitive. For all model types it was found that in general a three-mode minimal model could be identified that gave a reasonable approximation to the global prediction (including instabilities and regions of high sensitivity) but that the choice of which three modes was non-trivial.

A method of automatically selecting the modes of most significance for predictions at a particular bandwidth was identified and found to be highly effective for the simplest model that assumes infinite contact stiffness and neglects a velocity dependent coefficient of friction. The method also proved effective for models with finite contact stiffness and a velocity-dependent friction term for the values chosen. The method required selecting at least three of the most significant

modes for a given frequency of interest. Using two modes often resulted in unreliable predictions, which suggests that the hypothesised 'mode-coupling' route to instability based on only two modes may be too simplistic.

The analysis presented within this paper bridges the gap between reduced-order models and those of greater complexity. It is clear that there is a role for reduced-order models in making approximate predictions of a real system, but deriving a reliable minimal model is non-trivial. The method proposed for doing so has been shown to be effective for the system tested and may prove to be more widely applicable.

Acknowledgement

Financial support from the EPSRC is gratefully acknowledged.

References

[1] M.R. North, Disc brake squeal, *IMechE Conference on Braking of Road Vehicles*, 1976.
[2] R.A. Ibrahim, E. Rivin, Friction-induced vibration, chatter, squeal, and chaos part ii: Dynamics and modeling, *American Society of Mechanical Engineers Applied Mechanics Reviews* 47 (1994) 227–253.
[3] N.M. Kinkaid, O.M. O'Reilly, P. Papadopoulos, Automotive disc brake squeal, *Journal of Sound and Vibration* 267 (2003) 105–166.
[4] H. Ouyang, N. Nack, Y. Yuan, F. Chen, Numerical analysis of automotive disc brake squeal: a review, *International Journal of Vehicle Noise and Vibration* 1 (2005) 207–231.
[5] G. Sheng, *Friction-Induced Vibrations and Sound*, CRC Press, Boca Raton, FL, 2008.
[6] N. Coudeyras, J.-J. Sinou, S. Nacivet, A new treatment for predicting the self-excited vibrations of nonlinear systems with frictional interfaces: the constrained harmonic balance method, with application to disc brake squeal, *Journal of Sound and Vibration* 319 (2009) 1175–1199.
[7] R. Craig, M. Bampton, Coupling of substructures for dynamic analysis, *American Institute of Aeronautics and Astronautics—Journal* 6 (1968) 1313–1319.
[8] N. Hoffmann, M. Fischer, R. Allgaier, L. Gaul, A minimal model for studying properties of the mode-coupling type instability in friction induced oscillations, *Mechanics Research Communications* 29 (2002).
[9] N.M. Kinkaid, O.M. O'Reilly, P. Papadopoulos, On the transient dynamics of a multi-degree-of-freedom friction oscillator: a new mechanism for disc brake noise, *Journal of Sound and Vibration* 287 (2005) 901–917.
[10] U. von Wagner, D. Hochlenert, P. Hagedorn, Minimal models for disk brake squeal, *Journal of Sound and Vibration* 302 (2007) 527–539.
[11] M.N.A. Emira, Friction-induced oscillations of a slider: parametric study of some system parameters, *Journal of Sound and Vibration* 300 (2007) 916–931.
[12] O.N. Kirillov, Destabilization paradox due to breaking the Hamiltonian and reversible symmetry, *Journal of Non-Linear Mechanics* 42 (2007) 71–87.
[13] T. Butlin, J. Woodhouse, Sensitivity of friction-induced vibration in idealised systems, *Journal of Sound and Vibration* 319 (2009) 182–198.
[14] T. Butlin, J. Woodhouse, Sensitivity studies of friction-excited vibration, *International Journal of Vehicle Design* 51 (2009) 238–257.
[15] T. Butlin, Prediction and Sensitivity of Friction-Induced Vibration, Ph.D. Thesis, Cambridge University Engineering Department, 2007.
[16] P. Duffour, J. Woodhouse, Instability of systems with a frictional point contact. Part 1: basic modelling, *Journal of Sound and Vibration* 271 (2004) 365–390.
[17] J.J. Sinou, L. Jezequel, Mode coupling instability in friction-induced vibrations and its dependency on system parameters including damping, *European Journal of Mechanics A—Solids* 26 (2007).
[18] P. Duffour, J. Woodhouse, Instability of systems with a frictional point contact. Part 3: experimental tests, *Journal of Sound and Vibration* 304 (2007) 186–200.
[19] E.J. Skudrzyk, *Simple and Complex Vibratory Systems*, Pennsylvania State University Press, 1968.
[20] S.K. Wang, Characterisation of High-frequency Dynamic Friction, Ph.D. Thesis, University of Cambridge, 2008.
[21] R. Dorf, R. Bishop, *Modern Control Systems*, Addison-Wesley, Reading, MA, 1980.
[22] W.V. Nack, Brake squeal analysis by finite elements, *International Journal of Vehicle Design* 23 (2000).
[23] J.C. Huang, C.M. Krousgrill, A.K. Bajaj, An efficient approach to estimate critical value of friction coefficient in brake squeal analysis, *Journal of Applied Mechanics—Transactions of the ASME* 74 (2007).
[24] N. Hoffmann, L. Gaul, Effects of damping on mode-coupling instability in friction induced oscillations, *ZAMM—Journal of Applied Mathematics and Mechanics* 83 (2003).
[25] G. Fritz, J.J. Sinou, J.M. Duffal, L. Jezequel, Effects of damping on brake squeal coalescence patterns—application on a finite element model, *Mechanics Research Communications* 34 (2007).
[26] O. Giannini, A. Sestieri, Predictive model of squeal noise occurring on a laboratory brake, *Journal of Sound and Vibration* 296 (2006).